Chitosan, Gelatine, and Cellulose Based Hydrogels for the Removal of Potentially Toxic Elements from Aquaculture Water: A Comparative Study

ADVANCED SUSTAINABLE SYSTEMS
www.advsustainsys.com

Chitosan, Gelatine, and Cellulose Based Hydrogels for the Removal of Potentially Toxic Elements from Aquaculture Water: A Comparative Study

Monica Rigoletto, Rossella Sesia, Silvia Berto, Paola Calza, Marco Sangermano, Enzo Laurenti, and Mery Malandrino*

Since aquaculture is playing an increasingly important role in food supply, ensuring the healthiness of aquatic environments is a fundamental issue. Anthropogenic activities are often a source of contamination for water and, among the pollutants released, potentially toxic elements (PTEs) represent a well-known hazard to human health and ecosystem safety. In this study, carboxymethylcellulose-alginate (HY-ACMC), methacrylated-chitosan (HY-MCHI), and methacrylated-gelatine (HY-MGEL) hydrogels are synthesized, characterized, and tested as sorbents for PTEs removal. The removal efficiency is significantly affected by pH and contaminants' concentration. Furthermore, experiments in real aquaculture samples from Italy and Denmark farms are carried out to evaluate the matrix effect. Finally, hydrogel regeneration is optimized and sorbent efficiency for multiple cycles of water remediation treatment is investigated. All tested materials show promising removal capabilities even in real water. HY-ACMC has proven to be the most effective for single-cycle remediation treatments thanks to its high performance in all the studied conditions, although it is unstable to regeneration. On the other hand, regeneration with Na_2EDTA improves HY-MCHI efficiency, granting its prolonged employment over time. Considering both performances in real water samples and reusability results, HY-MGEL seems to be the most reliable material for multiple cycles of water remediation treatments.

1. Introduction

In the last seven decades' total fisheries and aquaculture production has significantly expanded with an annual growth rate of 3.3 percent. Aquaculture is one of the few sectors that maintained its growth trend also amid the worldwide spread of the COVID-19 pandemic, highlighting its importance since it contributes to fighting poverty, hunger, and malnutrition. Indeed, over half of aquatic food is farmed.[1]

In this context, a central theme is the preservation of the healthiness of water resources which may be subject to contamination due to a wide range of anthropic activities.

Among the various water contaminants, potentially toxic elements (PTEs) represent a well-known problem for ecosystem safety and for human health. Several sources of PTEs have been identified in aquaculture including industrial effluents, use of fertilizer and pesticides in agricultural activities, and finally contaminated feed for fish farming.[2]

PTEs are not biodegradable and can bioaccumulate in fishes, causing several pathologies, and biomagnify along the food chain.[3] For these reasons, there are many regulations that govern their use and limit their release in the environment worldwide.

Aquaculture-contaminated water can be treated by exploiting techniques developed for wastewater, including physical processes (reverse osmosis, filtration, membrane technique, flotation, coagulation-flocculation), chemical (precipitation, ion exchange, electrochemical, reduction/oxidation treatments) and biological methods. However, these techniques could be very expensive and sometimes not effective at pollutants low concentrations.[2]

Adsorption is one of the most studied techniques for PTEs contaminated water remediation and has some advantages compared to other strategies: adsorbent materials are relatively cheaper, can be derived from agro-industrial wastes, regenerated, and used for subsequent adsorption-desorption cycles.[4]

Among the existing adsorbents, those deriving from natural and renewable resources have recently received growing interest since they represent available and low-cost materials with a limited environmental impact. Hence, they could be considered promising alternatives to classic water remediation

M. Rigoletto, S. Berto, P. Calza, E. Laurenti, M. Malandrino
Department of Chemistry
Università degli Studi di Torino
Via Pietro Giuria 7, Torino 10125, Italy
E-mail: enzo.laurenti@unito.it
R. Sesia, M. Sangermano
Department of Applied Science and Technology
Politecnico di Torino
Corso Duca degli Abruzzi 24, Torino 10129, Italy
The ORCID identification number(s) for the author(s) of this article can be found under https://doi.org/10.1002/adsu.202400933

DOI: 10.1002/adsu.202400933

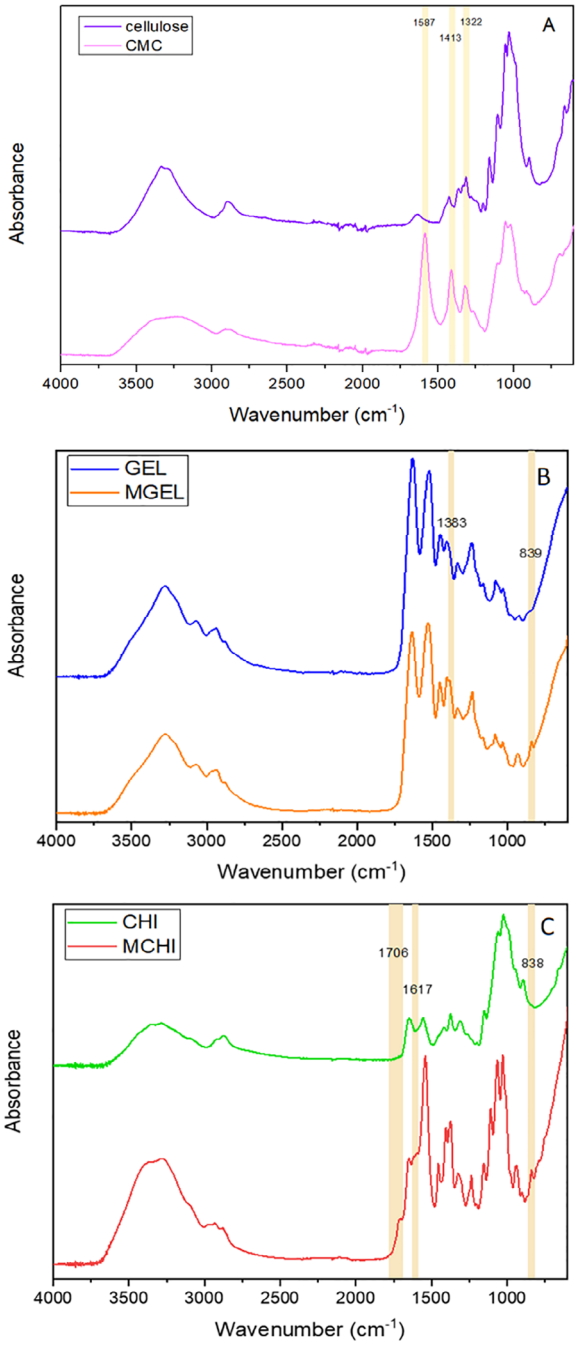

Figure 1. ATR-FTIR spectra of pristine and functionalized materials: A) comparison between cellulose and carboxymethyl cellulose (CMC); B) comparison between gelatine (GEL) and methacrylated gelatine (MGEL); C) comparison between chitosan (CHI) and methacrylated chitosan (MCHI).

strategies. Within this context, biopolymers-based hydrogels emerge as noteworthy materials for PTEs uptake. Hydrogels are 3D networks with high swelling properties in water due to the presence of hydrophilic groups in the polymeric structure, such as hydroxyl, amino, or carboxylic ones. The adsorption phenomenon is based on physicochemical interaction between adsorbent's functional groups and PTEs' species present in solution. The most common mechanisms of biosorption include electrostatic interactions as well as ion exchange, complexation, chelation, coordination, and hydrogen bonding. These interactions, and consequently the PTEs removal efficiency, are affected by experimental conditions such as pH, temperature, and pollutant concentration.[5] Therefore, properly designing materials and setting up tests are fundamental.

Although natural polymers such as cellulose, alginate, chitosan, and gelatine contain chemical groups capable of interacting with PTEs, it is often necessary to introduce new functionalities to improve their affinity toward these contaminants. Furthermore, specific functional groups are required to enable the cross-linking process to obtain the hydrogel structure.[6–10]

Experimental conditions could also affect the stability of the adsorbent depending on the type of hydrogel prepared. Physically cross-linked hydrogels, also known as reversible gels, are easily formed due to weak interactions between polymer chains that occur after the introduction of gelling ions. For example, mannuronic and glucuronic blocks of alginate can be cross-linked exploiting the ionic interaction with Ca^{2+} ions.[11] Since this kind of network can be destroyed in the presence of non-gelling cations such as Na^{+}, physically cross-linked natural hydrogels could possess lower stability and poorer mechanical properties with respect to other materials. To overcome these drawbacks, permanent hydrogels could be obtained by forming covalent bonds in the hydrogel matrix.[12] An interesting strategy to obtain chemical cross-linked hydrogels is the UV-curing. This eco-friendly polymerization technique involves neither the use of solvents nor the production of waste and is very fast, thus saving energy.[13–15] An appropriate functionalization of the natural polymer allows the formation of covalent bonds between polymer chains under UV-light irradiation following the addition of a photoinitiator.[10]

In this work, we methacrylated gelatine (MGEL) and chitosan (MCHI) and then exploited radical photopolymerization to prepare hydrogels based on gelatine (HY-MGEL) and chitosan (HY-MCHI) in water at room temperature.[8,16] Meanwhile, we prepared physically cross-linked hydrogels containing alginate and carboxymethylcellulose (HY-ACMC) previously obtained by chemically modifying waste-deriving cellulose.

All prepared hydrogels have been characterized and tested for the removal of a mixture of seven PTEs (copper, lead, cadmium, nickel, zinc, arsenic, and mercury) in both ultra-pure and aquaculture spiked water. The influence of pH and pollutant's initial concentration have been evaluated as well as the matrix effect.

Furthermore, we optimized hydrogel regeneration treatment and investigated the reusability of our materials for several subsequent adsorption-desorption cycles.

2. Results and Discussion

2.1. Characterization

Attenuated total reflectance-infrared spectroscopy (ATR-FTIR) was used to confirm the functionalization reactions of the bio-based precursor polymers cellulose, chitosan, and gelatine. **Figure 1** shows ATR-FTIR spectra of all the pristine and chemically modified materials employed for the hydrogel synthesis.

Table 1. Swelling and point of zero charges (PZC) values for synthesized hydrogels.

	Sw_{eq}	PZC
HY-ACMC	2.2	<3
HY-MGEL	2.1	4.4
HY-MCHI	6.5	6.4

Cellulose and carboxymethylcellulose (CMC) spectra are compared in Figure 1A. The carboxymethylation reaction of cellulose ensures the biopolymer's water solubility. The carboxymethyl group introduction is clearly confirmed by the presence of three characteristic peaks in the CMC spectrum: 1587 and 1413 cm^{-1} signals are ascribed to the asymmetric and symmetric COO^- stretching, while the peak at 1322 cm^{-1} is related to C—O bending vibration.[17]

On the other hand, for HY-MGEL and HY-MCHI preparation the incorporation of methacrylic groups is crucial to UV-cure gelatine and chitosan. In Figure 1B the ATR-FTIR spectra of GEL before and after the functionalization are reported. As can be clearly noted in the MGEL spectrum, two new peaks appeared at 1383 and 839 cm^{-1}, they can be assigned to the C—O stretching and C═C bending vibrations, respectively.[18] In Figure 1C the spectra of CHI and MCHI are compared. Also, in this case, the appearance of new signals in the MCHI spectrum suggested the achievement of the methacrylation reaction. In particular, the introduction of the methacrylic groups was confirmed in the MCHI spectrum by the presence of the signal at 1706 cm^{-1}, attributable to the C═O stretches, and the signals at 1617 and 838 cm^{-1}, assignable to the C═C stretching and bending vibrations, respectively.[19]

After functionalization (the substitution degree is reported in Table S1, Supporting Information) either physical or chemical cross-linked hydrogels were prepared and their swelling capabilities were assessed by a gravimetric measure. Figure S1 (Supporting Information) shows the increase in weight as a function of the contact time with ultrapure water for HY-ACMC, HY-MCHI, and HY-MGEL, while the Sw values at the equilibrium state are reported in **Table 1**. HY-MCHI shows a superior swelling capability with a Sw_{eq} of 6.5 achieved in less than an hour of immersion in water, coherent with data previously reported in the literature for the same material.[18] HY-MGEL and HY-ACMC present similar behavior with Sw_{eq} values of 2.1 and 2.2 respectively, reaching the equilibrium in ≈4 h (Figure S1, Supporting Information).

Another important aspect is the ionic state of the hydrogels' surface that plays a crucial role in the interactions with metal ions and depends on pH. The surface charge as a function of pH values was investigated by means of the ζ potential measurement. The HY-MGEL's surface charge was proved to be strongly affected by pH with a point of zero charge (PZC) around 4.4 (Table 1).[18,20–23] Noè et al.[18] performed ζ potential analysis on methacrylated gelatine and demonstrated that under acidic conditions HY-MGEL possesses a positively charged surface due to the protonation of its amino groups. On the other hand, at pH values >4.4, its surface charge becomes negative because of the functional groups' deprotonation.[18,20] The same trend of ζ potential was also found for HY-MCHI with a PZC at a pH of ≈6.4, as suggested by chitosan pKa of 6.5. Therefore, in acidic conditions, the HY-MCHI amino groups are protonated causing a positive charge of the surface, while the HY-MCHI exhibits negative ζ potential as pH increases due to the deprotonation of hydroxyl groups.[18,19,24,25]

Furthermore, the protonated amino groups cause an electrostatic repulsion among the HY-MCHI's polymeric chains, making the hydrogel chemically and mechanically unstable.[19] As suggested by the measurement of the ζ potential, both HY-MGEL and HY-MCHI exhibit an amphoteric nature.[23,26–33]

The ζ potential analysis of HY-ACMC hydrogels (Figure S2, Supporting Information) evidenced a negative surface charge throughout the pH range studied (3-7) with a tendency to increase as acidity increases. This trend suggests a PZC at pH<3 (Table 1) and is in agreement with several studies that reported similar results for both sodium alginate and carboxymethyl cellulose.[34–36] Indeed, both these biopolymers contain carboxylate and show pKa values between 3.5 and 3.7.[34,37] Therefore, since the pH range studied is above the pKa, the functional groups are deprotonated, resulting in a negative surface charge.

The ζ potential values of these adsorbents at different pH together with the PTE chemical speciation are crucial factors to understand the adsorption process.[38]

2.2. PTEs Adsorption Tests in Ultrapure Water

HY-ACMC, HY-MGEL, and HY-MCHI have been tested for PTEs' removal from aqueous matrix. To clarify the adsorption behavior of each material, experiments were conducted at different initial PTEs concentrations and pH values.

The influence of initial PTEs concentration was studied through adsorption tests carried out at pH 5 in 10^{-6}, 10^{-5}, and 10^{-4} M multi-element solutions (complete removal curves as function of contact time are reported in Figure S3, Supporting Information). As reported in **Figure 2**, both HY-ACMC and HY-MGEL show good removal percentages (R%) for most of the studied elements after 24 h of treatment. In particular, HY-ACMC hydrogel leads to R% > 95% for Pb and ≥75% for Cu and Cd for all the PTEs' initial concentrations studied.

Gelatine-based hydrogel adsorption capacity is more affected by elements' concentration. Indeed, HY-MGEL shows decreasing R% of Zn (96%; 54%, and 6%) going from 10^{-6} to 10^{-4} M and a similar behavior can be noted also for Cd and Ni. On the contrary, passing from 10^{-6} to 10^{-5}M Cu and Pb R% increases to decrease again at 10^{-4} M. The latter two elements seem to be the most affected by the competition for the hydrogel's active sites. According to Table S2 (Supporting Information), they are among the elements with the largest ionic radius and thus characterized by a lower charge density. Moreover, HY-MGEL is a permanent hydrogel, meaning that its network is made up of covalent bonds which make it more stable but at the same time probably less suitable for ionic exchange. The combination of these two factors can affect Pb and Cu removal. However, for all investigated concentrations, a removal percentage >40% for most contaminants is ensured.

On the other hand, HY-MCHI shows a high specificity for Hg which is removed between 45% and 90% as a function of initial concentration. The R% of other PTEs are significantly lower

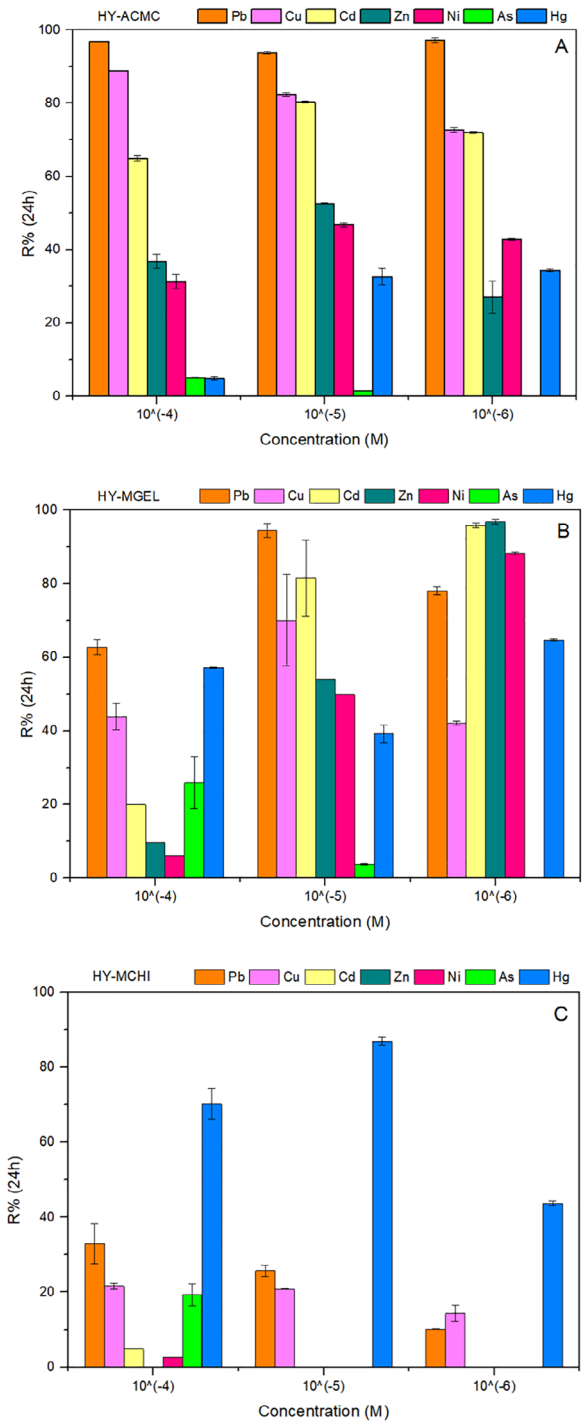

Figure 2. Removal percentages after 24 h of contact with 1g L^{-1} of adsorbent as a function of PTEs concentration: A) HY-ACMC; B) HY-MGEL; C) HY-MCHI.

with respect to those of mercury and increase passing from 10^{-6} to 10^{-4} M. It can be assumed that a higher initial concentration promotes competition for the HY-MCHI active sites.

It is clear that the hydrogel adsorption behavior toward the investigated contaminants depends on multiple factors, such as competition effects between the elements, their speciation at pH 5, and the steric hindrance and charge density of their aquaions.

Due to the complexity of these mechanisms and their combined effect, a defined common trend for all the elements with increasing concentration is not observable. Overall, an increasing trend in the adsorption of PTEs as their concentrations decrease can be generally observed for HY-ACMC and HY-MGEL, while for HY-MCHI other factors are involved.

To evaluate the possible use of hydrogels in an aqueous matrix with different acidity levels, adsorption tests were carried out at different pH values (3.5, 5, and 7) maintaining an initial PTEs concentration of 10^{-5} M.

The solution pH affects not only the surface charge of the materials, as demonstrated by ζ potential measurements, but also PTEs speciation (Figure S4, Supporting Information). Therefore, both these factors influence the adsorption phenomenon since they determine the interaction between adsorbate and adsorbent.[38]

Figure 3 summarizes the removal percentages obtained after 24 h of contact for HY-ACMC (Figure 3A), HY-MGEL (Figure 3B), and HY-MCHI (Figure 3C), while the complete adsorption curves as a function of contact time are reported in Figure S5 (Supporting Information).

HY-ACMC shows similar adsorption capacities throughout the studied pH range. This behavior agrees with ζ potential, which is negative for all the pH studied with decreasing values, corresponding to an increase in surface negative charges, as the alkalinity of the solution increases (Table 1; Figure S2, Supporting Information). This allows HY-ACMC to establish an electrostatic interaction with metals in cationic form or as positively charged hydrolytic species. Indeed, the highest removal percentages for HY-ACMC were found for Pb, Cu, and Cd, which are predominantly present as Pb^{2+} or $Pb(OH)^{+}$, Cu^{2+}, and Cd^{2+} in the pH range 3.5–7 (Figure S4, Supporting Information). Although Figure 3 A shows a selectivity in the removal of Pb, Cu, and Cd, R% for Zn and Ni are not negligible (≈30–50%) since they are present as divalent cations and can be adsorbed through electrostatic interactions.

The removal trend (Pb > Cu > Cd >> Zn ≥ Ni) is the result of a competition for the surface adsorption sites of HY-ACMC and can be related to the metallic ions properties such as electronegativity, ionic radius, and charge density. Considering Pb, Cu, Cd, and Zn, the affinity for HY-ACMC matches with Pauling's electronegativity order (Pb 2.33; Cu 1.9; Cd 1.69, and Zn 1.65), with the reverse order of hydrated ionic radius (Pb 4.01 Å; Cu 4.19 Å; Cd 4.26 Å, and Zn 4.3 Å) and consequently of the charge density. These trends are in agreement with those reported in similar studies regarding metal ions competitive removal.[39–41]

Furthermore, another crucial factor to explain the competitive adsorption is the stability constant of the metal-ligand complexes, which in HY-ACMC hydrogels are represented by metal – carboxylate (acetate) complexes:

$$M^{n+} + -COO^{-} \leftrightarrow M(COO)^{n-} \quad (1)$$

As reported in Table S2 (Supporting Information), the logK values for Pb, Cu, Cd, Zn, and Ni are 2.58, 2.21, 1.92, 1.57, and 1.44,

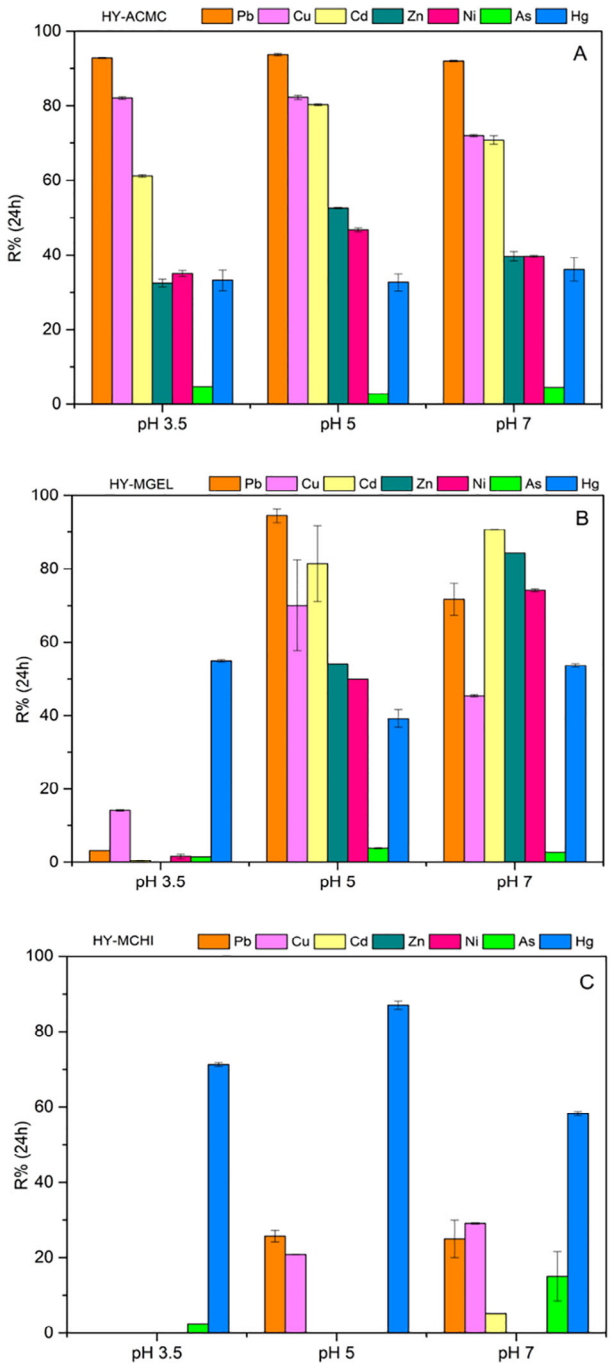

Figure 3. Removal percentages after 24 h of contact with 1g L^{-1} of adsorbent as function pH: A) HY-ACMC; B) HY-MGEL; C) HY-MCHI.

respectively (NIST SDR 96 Database (t = 25 °C, I = 0)), which perfectly reflect the removal order found experimentally[40].

Furthermore, it was found that in neutral conditions a longer time was required to reach the equilibrium state, from ≈4 h at pH 3.5 and 5 to 5 h at pH 7 (Figure S5, Supporting Information). Pb and Cu are removed by HY-ACMC with similar kinetics at pH 3.5 and 5 since they are in the form of aquaions. Instead, at pH 7 the species $Pb(OH)^+$, $Cu(OH)^+$ and $Cu(OH)_{2(s)}$ are also present (Figure S4, Supporting Information) reducing the amount of aquaions and leading to a slightly lower R% after 24 h of treatment.

Unlike HY-ACMC, HY-MGEL shows very low or no effectiveness in removing the majority of the PTEs at pH 3.5 (Figure 3B). As can be detectable from the ζ potential measurements, the gelatine-based material has a positive surface charge at pH 3.5 (PZC = 4.4, Table 1). Therefore, the protonation of HY-MGEL's amino groups causes electrostatic repulsion toward metal cations, making their adsorption difficult.

Instead, as alkalinity increases, the HY-MGEL surface becomes negatively charged due to the deprotonation of hydroxyl groups and hence more available to establish attractive electrostatic interactions with metallic cations. Indeed, at pH 5 Cu^{2+} and Pb^{2+} are the predominant species in the aqueous solution (Figure S4, Supporting Information) and can be adsorbed on HY-MGEL through electrostatic bonds. However, Pb and Cu R% values slightly decrease at pH 7 (Figure 3B) since also $Pb(OH)^+$, $Cu(OH)^+$, and $Cu(OH)_{2(s)}$ are present (Figure S4, Supporting Information), highlighting a HY-MGEL's selectivity toward divalent metallic cations. As noted before for HY-ACMC, the competitive adsorption outcomes depend also on the PTEs' ionic radius and the relative charge density since species with less charge and larger size, such as $Pb(OH)^+$ and $Cu(OH)^+$, lead to less stable complexes.[42] Therefore, the reduced R% of Pb and Cu found at pH 7 is justified.

Furthermore, as shown in Figure 3B, a linear trend of R% for Cd, Zn, and Ni as a function of pH is noteworthy: Cd > Zn > Ni. Considering that they are present as Cd^{2+}, Zn^{2+}, and Ni^{2+} in all the pH ranges investigated, the removal sequence could be related to a sum of factors including the electronegativity, charge density, and affinity for surface functional groups (amino or hydroxyl groups, and amide functionalities). Moreover, this R% trend has been reported in different studies carried out employing materials containing the same moieties.[43–45]

As well as HY-MGEL, also HY-MCHI is not effective in removing the PTEs at pH 3.5, while at pH 5 and 7 it ensures an R% between 20% and 30% for Cu and 25% for Pb after 24 h of contact time. On the contrary, Cd, Zn, and Ni are not removed by HY-MCHI throughout the pH range examined (Figure 3C). The minor adsorption capacity of HY-MCHI can be explained by considering its positive surface charge at pH values below its PZC (Table 1), which produces electrostatic repulsion toward metals in cationic form or positively charged aquoion species. However, as can be noted in Figure 3C, HY-MCHI has a remarkably high removal efficiency for Hg present in the multi-element solution. Hg is mainly present in solution as a neutral hydrolytic species therefore no electrostatic repulsion occurs (Figure S4, Supporting Information). Moreover, in this condition electron pair of chitosan's nitrogen atoms can be available for the complex formation with the metal ions.[46] The R% for this element reaches ≈90% at pH 5 and maintains values higher than 60% at pH 3.5 and 7. This trend is in agreement with the results obtained by Dubey et al.[46] and Monier et al.[47] who highlighted that as the solution's pH increases, the number of Hg ions removed also increases with optimum adsorption at pH 5. At strong acidic pH values, the abundant presence of H^+ and H_3O^+ ions could compete with Hg for the adsorption sites affecting the treatment outcomes and making the amine groups less available for the metal

ion coordination.[46–48] While at pH>5 the decreased Hg retention and the increased R% for other PTEs could be due to hydrolytic equilibria competition.[46]

Finally, to analyze the limited effectiveness of arsenic removal by HY-ACMC, HY-MGEL, and HY-MCHI, the As speciation needs to be considered. According to the equilibrium dissociation constants, the arsenate species are negative at pH>2.2.[18,49] Therefore, as mentioned above, HY-ACMC removes As with R%<10% due to its negatively charged surface (Figure S2, Supporting Information), which causes an electrostatic repulsion toward the arsenic species (Figure 3A). Although HY-MGEL shows a positive ζ potential at pH<4.4, the As removal is insignificant at pH 3.5 (Figure 3B), since the HY-MGEL's carboxylic groups can interact with amino groups of the structure.[18,50,51] As well as HY-ACMC, also HY-MGEL's negative surface charges hinder the As adsorption at pH higher than its PZC (Figure 3B). By contrast, HY-MCHI proves better at removing As especially at neutral pH (Figure 3C), where $H_2AsO_3^-$ is the predominant species.[49] At this pH, HY-MCHI still shows a partially positive surface charge (Table 1) and a balance between the surface amino groups' charge and the distance between the polymeric chains.[18] These factors allow the chitosan-based hydrogel to remove arsenic with an R% at ≈15% (Figure 3C).

2.3. PTEs Adsorption Tests in Real Aquaculture Water

To study the behavior of the synthesized hydrogels in real conditions, two water samples from aquaculture farms were employed as a matrix for the preparation of the multi-element solutions.

Before usage, these water samples were characterized by analyzing natural PTEs content, hardness, and acidity. Table S3 (Supporting Information) reports characterization results and Italian legal limits concentration for all studied elements. For Italian koi-carps' aquaculture water the hardness, expressed in mg L^{-1} of $CaCO_3$, was 98.06 and it presented a pH value of 8.03. Danish water was characterized by a hardness of 194.71 and a pH of 7.76. Both samples displayed very low concentrations of PTEs, so spikes of each element were necessary to perform adsorption experiments. As reported in paragraph 2.7, these experiments have been carried out at concentrations near the Italian legal limit (50 µg L^{-1} As; 22 or 40 µg L^{-1} Cu; 10 or 20 µg L^{-1} Pb; 50 or 75 µg L^{-1} Ni and 200 or 300 µg L^{-1} Zn, as reported in Table S3, Supporting Information) as a function of water hardness (Italian Legislative Decree n°152/2006, Annex 2, Part III, Section B). Instead, Cd and Hg were introduced with a concentration of 5 µg L^{-1} which is higher than their legal limit (2.5 and 0.5 µg L^{-1}, respectively).

Figure 4 summarizes R% values obtained with HY-ACMC, HY-MGEL, and HY-MCHI after 180 min of contact with PTEs multi-element solution prepared in the two aquaculture water samples. Complete adsorption curves are reported in Figure S6 (Supporting Information).

Regarding the koi-carps' spiked water, HY-ACMC hydrogels ensure a sufficient R% to bring all the pollutant concentrations below the legal limits except for copper and arsenic. As evidenced in Figure 2A, HY-ACMC shows a PTEs removal behavior not significantly affected by the pollutant's initial concentrations. This suggests that the inhibition of Cu removal could be ascribable

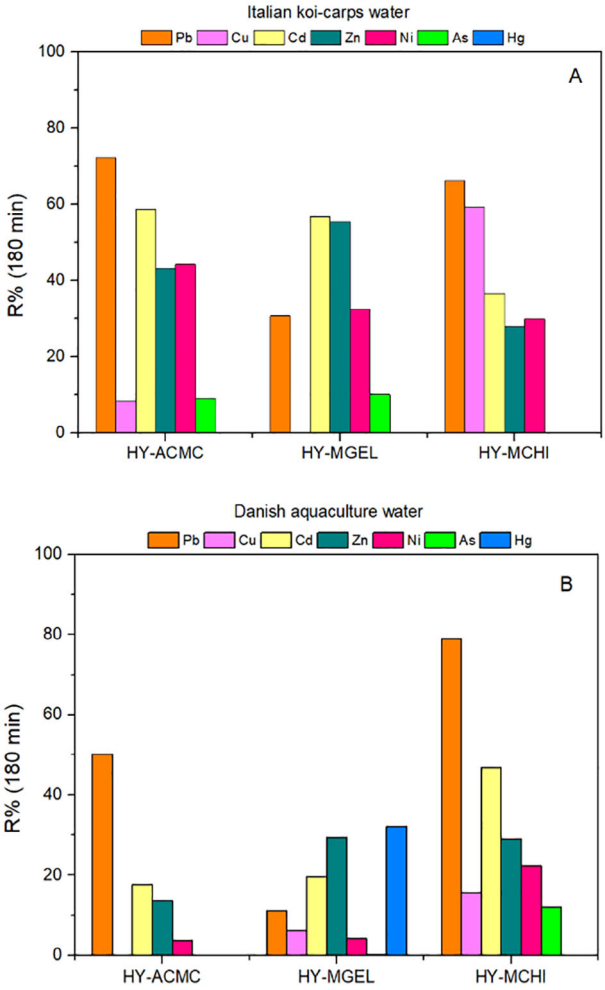

Figure 4. Removal percentages after 180 min of contact with 1 g L^{-1} of adsorbent in A) Italian koi-carps spiked water and B) Danish aquaculture spiked water.

to its speciation. Indeed, at pH 8 the main species in solution is $Cu(OH)_{2(s)}$, which is neutral, while the concentration of the aqua-ion form is negligible.

Furthermore, Cu can be strongly complexed by dissolved organic matter, in particular by humic acids (HA), forming soluble complexes, which reduce its availability for adsorption. Esfandiar et al.[52] studied the influence of humic acid on different metal speciation and reported as, at high organic matter concentration (20 mg L^{-1}), the metal-HA complexes represented the main species in solution for Cu and Pb. On the other hand, Zn, Ni, and Cd's speciation showed to be less affected by the presence of HA. This is consistent for koi-carps' water as the organic carbon content was 150 mg/L, as previously evaluated by a non-purgeable organic carbon (NPOC) analysis.[53]

On the other hand, since As is in anionic form and the surface of the HY-ACMC is negative at aquaculture water pH (7.7–8.1), the repulsion between the charges justifies the limited removal of this contaminant. As in ultra-pure water experiments, the most removed PTEs are Pb and Cd with R% values of 72% and 59%, respectively.

HY-MGEL is effective in the concentration reduction below the legal limits for most of the elements studied with removal percentages between 30 and 56%. As (R% <10%) and Cu (R% = 0%) are not removed sufficiently to return within legal limits. As for HY-ACMC, also in this case the speciation of copper and arsenic, the HA-metal complexes formation, and the surface charge of the material can explain the poor R% obtained for these two PTEs.

Finally, although in general HY-MCHI removal capacity is inversely proportional to the contaminant initial concentration (Figure 2C), it shows a good removal capacity for most of the PTEs investigated, except for As and Zn, leading to a sufficient removal percentage to bring them below the concentration legal limits. Indeed, Pb and Cu are removed more than 60%; Cd ≈40% and Ni 35%. Despite the low PTEs concentration (10^{-7} M) these R% values are probably related to the water pH, which is ≈8 and is higher than HY-MCHI PZC ensuring a negatively charged surface of the material and a better removal capacity.

As shown in Figure 4B, in Danish aquaculture water HY-ACMC and HY-MGEL show lower removal capabilities in respect to those obtained in the previous aquaculture water sample. It is important to consider that in this case there was a higher content of salts since the hardness is 194.71 mg L^{-1}. Cations such as K^+, Na^+, Ca^{2+}, and Mg^{2+} could compete with other aquaions for material surface active sites affecting their R%. Several studies[44,52,54] concerning the influence of environmental factors on PTEs competitive adsorption reported that natural divalent cations show a higher inhibition effect on metal ions removal compared to the monovalent ones according to the trend Mg^{2+}>Ca^{2+}>K^+. Indeed, in the treatment with HY-ACMC the R% more reduced are those of Cd (from 60% to 17%), Zn (from 43% to 13%), and Ni (from 45% to 4%). All of them at a pH of 7.76 (Danish water pH value) are mainly present in solution as bi-charged cations (Figure S4, Supporting Information). On the other hand, in these conditions, Pb is in the form of aquaions and of mono-charged cation ($Pb(OH)^+$), hence its R% undergoes a smaller reduction.

Similar behavior is evidenced for HY-MGEL, which shows a lower removal capacity for all the PTEs studied except mercury. Indeed, Cd and Pb show removal percentages at ≈35% of those in koi-carps' water, Zn ≈50%, and Ni 13%.

As for the koi-carps sample, also in this case HY-MCHI shows a better efficiency in removing contaminants compared to pure water, similar to those obtained in the previous real sample.

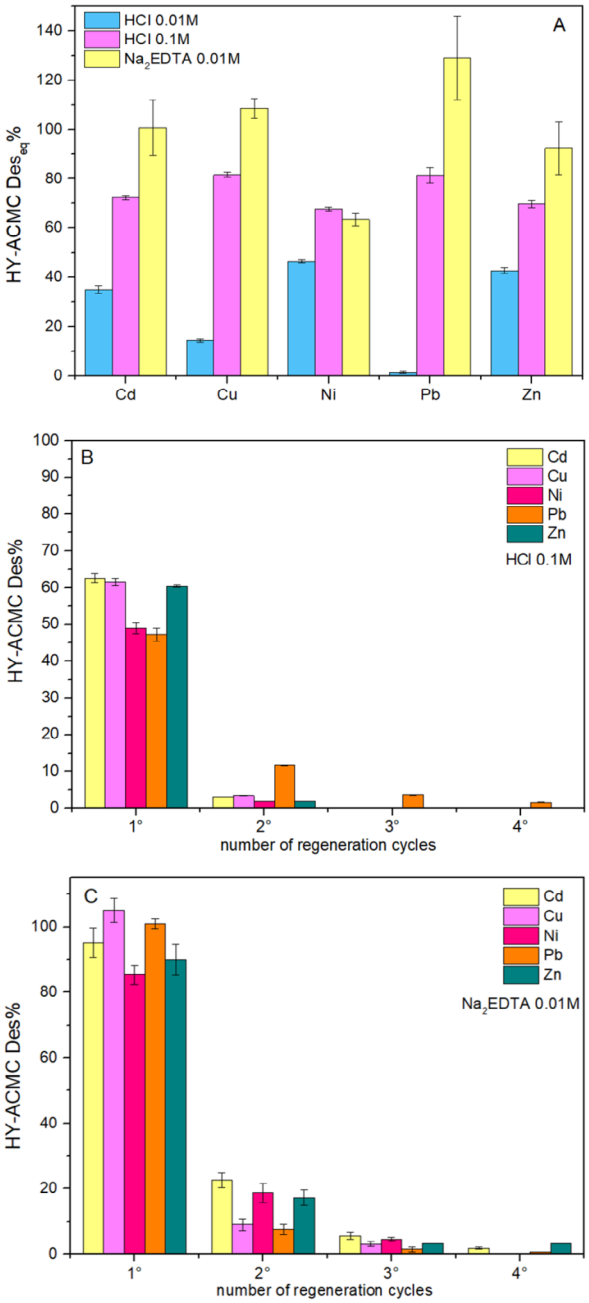

Figure 5. Percentage of PTEs desorption from HY-ACMC hydrogels A) with different regeneration solutions; B) with subsequent cycles of regeneration with HCl 0.1 M; C) with subsequent cycles of regeneration with Na_2EDTA 0.01 M.

2.4. Hydrogels Regeneration and Reuse

Preliminary regeneration tests have been done on HY-ACMC hydrogels. According to existing literature, three different regeneration solutions have been tested: HCl 0.01 and 0.1 M[19,55] and Na_2EDTA 0.01 M.[56] **Figure 5A** displays the desorption percentages at the equilibrium state of HY-ACMC in the three regeneration solutions. HCl 0.01 M solution leads to a release of less than 50% for all elements studied and is ineffective for Pb desorption, while increasing HCl concentration to 0.1 M the percentage of desorption rises between 70% and 80%. The best regeneration solution was Na_2EDTA 0.01 M as ensures a complete desorption for all the PTEs except for Ni, which is however released for 65%. This effectiveness is related to the Na_2EDTA high complexing capacity toward PTEs as evidenced by the complexation constants reported in Table S4 (Supporting Information).

Figure 5B,C summarize the desorption percentages obtained using HCl 0.1 M and Na_2EDTA 0.01 M for subsequent regeneration cycles each lasting 30 min.

In the first two desorption cycles with HCl 0.1 M PTEs release is between 50% and 60% and it is not significant in the third and fourth cycles. Pb is released in all regeneration cycles with a percentage of still 1.5% in the fourth one. Regeneration treatment

with HCl 0.1 M ensures a total release ≈70% for Cd, Cu, and Pb, 65% for Zn, and 55% for Ni.

Employing Na_2EDTA 0.01 M as a regeneration solution, a desorption percentage higher than 85% is achieved for all PTEs in the first cycle, between 10% and 20% in the second one and it decreases under 10% and then near 0% in the last two cycles.

This regeneration treatment ensures a complete release for all investigated elements. The higher percentages of PTEs desorption, the lower concentration, and the not excessive acidity of the solution led to the selection of Na_2EDTA 0.01 M as the most promising regeneration treatment. Then, HY-ACMC, HY-MGEL, and HY-MCHI were reused for different subsequent PTEs adsorption tests interspersed with 0.01 M Na_2EDTA regeneration treatments.

Each regeneration treatment included only 3 desorption cycles as the releases of the fourth one were found to be not significant.

Figure 6 and Table S5 (Supporting Information) summarize the results of PTEs adsorption-desorption cycles obtained with the three hydrogels.

Desorption values include the total releases obtained with all three 30-minute' cycles that make up each regeneration treatment. Between each adsorption and desorption process, hydrogels have been washed with ultrapure water. PTEs concentrations in washing water were also evaluated and were not significant in all the regeneration treatments except for HY-ACMC, probably due to the breakdown of its network.

Indeed, Figure 6A reports the results of only two adsorption-desorption cycles obtained with HY-ACMC which proves to be less resistant than other materials. As previously reported, the physical cross-linking stability is affected by the presence of monovalent metal cations in solution. During the regeneration in Na_2EDTA solution, sodium ions can substitute calcium ions in the hydrogel network, partially compromising the integrity of the structure.[11,57] This can affect HY-ACMC's PTEs removal efficiency, which is reduced by >65% after the first regeneration treatment. Furthermore, some surface sites could be involved in the coordination of sodium ions and are no longer available for the removal of PTEs. Moreover, the desorption percentages obtained in the second regeneration treatment are very low, probably also due to the damage of the hydrogel polymeric network that makes subsequent uses very difficult.

As shown in Figure 6B, HY-MGEL shows a good PTEs removal capacity in the first adsorption cycle which decreases in the second and the third ones for Zn, Cd, and Ni. Pb and Cu removals are reduced in the second cycle while increasing again in the third one. Hg adsorption efficiency remains almost constant in the first two cycles and decreases only in the third one. Regarding the regeneration process, desorption is not complete in all cycles for most of the studied PTEs (<65%) and initially decreases from the first to the second cycle and then rises again in the third one. Only for Ni and Zn in the last regeneration treatment full release is achieved.

HY-MCHI increases its adsorption capacities going from the first to the second cycle of PTEs removal and the efficiency is maintained also in the third cycle. It is noteworthy that the first regeneration treatment allows the adsorption of elements first not removed like Cd, Cu, Ni, and Zn. It can be assumed that during the desorption treatment, the excess of Na_2EDTA not involved in metal ions complexation could enter the HY-MCHI polymeric

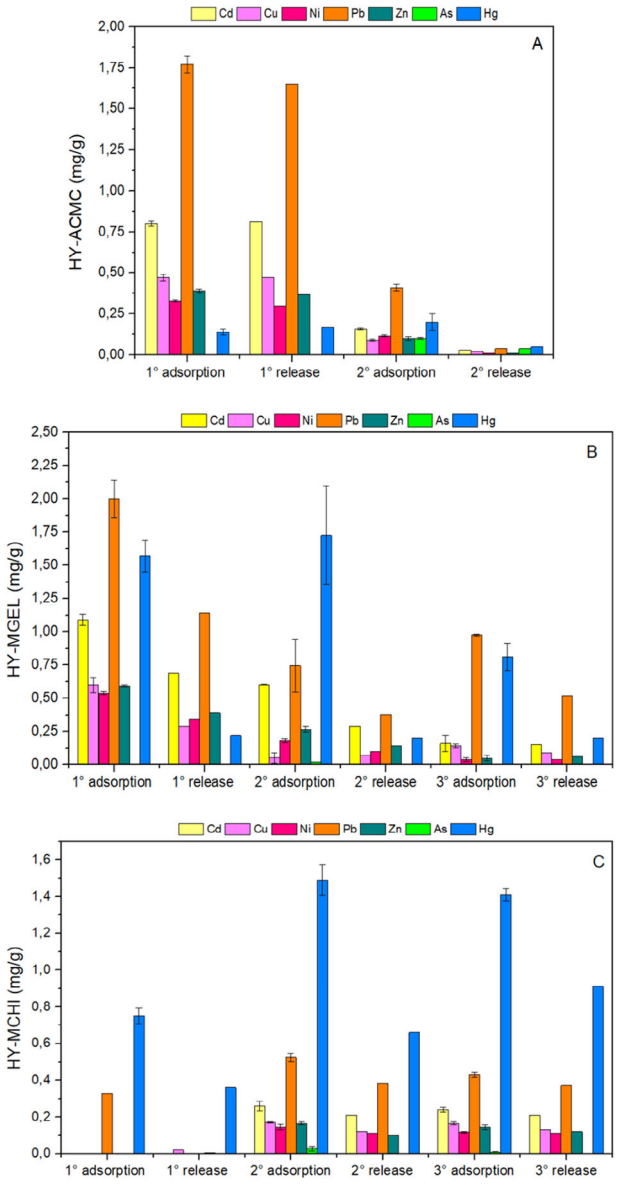

Figure 6. PTEs adsorption (after 180 min of contact with adsorbent materials) and releases obtained with Na_2EDTA 0.01 M, expressed in mg g^{-1}, in a subsequent cycle of reuse. A) HY-ACMC; B) HY-MGEL; C) HY-MCHI.

structure and interact electrostatically with chitosan. Indeed, at the pH of the regeneration solution (pH 4.6), the amino groups of HY-MCHI are protonated and positively charged while Na_2EDTA shows two carboxylate groups negatively charged (pKa 2.0, 2.7, 6.2, and 10.3[58]). This electrostatic interaction remains also in the subsequent PTEs adsorption experiments since they were carried out at pH 5. The entrapped $EDTA^{2-}$ can act as a chelating agent increasing the number of HY-MCHI active sites available for PTEs adsorption. This statement can be confirmed by comparing the PTEs removal percentages with the trend of the stability constants reported for EDTA-metal complexes (Table S4, Supporting Information).[59]

Regeneration treatments of HY-MCHI are effective for all PTEs adsorbed with releases between 60% and 85% except for

Hg which interacts strongly with hydrogel's surface, and which is desorbed ≈50%.

Although it is complex to make a meaningful comparison with other materials described in recent studies due to the exploitation of different concentrations of contaminants and adsorbent materials, the influence of diverse environmental factors must be considered. Indeed, in Table S6 (Supporting Information) a summary of the existing literature concerning the materials' reusability and a comparison with our results is reported.

The number of cycles carried out with the hydrogels developed in this work is in line with the studies in the literature about the removal of mixtures of PTEs, although in some cases a lower loss in efficiency was reported. It is worth emphasizing that in most published papers the materials' adsorption capabilities are evaluated in a bi- or tri-element mixture. On the contrary, in this study, we considered solutions containing 7 PTEs, which imply more competition mechanisms for the surface sites. This leads to an increase in the complexity of the adsorption-desorption processes that can result in a reduction of efficiency.

3. Conclusion

This work aims to evaluate the removal of seven PTEs (Pb, Cu, Cd, Ni, Zn, Hg, and As) from both ultra-pure water and spiked aquaculture water using three different hydrogels obtained from biomasses: carboxymethylcellulose-alginate hydrogels (HY-ACMC), prepared through gelation process, and methacrylated chitosan (HY-MCHI) and gelatin (HY-MGEL) hydrogels, produced via photopolymerization.

Hydrogels have been deeply characterized, and their removal capabilities as a function of the initial concentration of contaminants and the pH of the solution have been studied, as well as their reusability.

The investigations about the pH-dependent removal have demonstrated that PTEs' adsorption is influenced by the acidity of the systems due to the pH effect on the adsorbents' surface ionic state, particularly for HY-MCHI and HY-MGEL, and on PTEs speciation. Overall, all tested materials showed promising removal capabilities also in actual waters.

HY-ACMC has proven to be the most effective for single-cycle water remediation treatments since its good performances are not significantly affected by all the factors considered. However, it cannot be easily regenerated as it shows an intrinsic structural instability.

On the other hand, in ultra-pure water, HY-MCHI shows reduced adsorption capacity for all PTEs, except for mercury. However, regeneration with Na_2EDTA improves its removal capabilities toward all PTEs, granting its prolonged efficiency over time. The introduction of an activation step with Na_2EDTA could be also considered to increase HY-MCHI efficiency in the first cycle of use.

However, considering both performances in real water samples and reusability, HY-MGEL seems to be the most reliable material for multiple water remediation treatments.

To conclude the evaluation of the possible use of these sustainable biomass-based materials in real situations it will certainly be necessary to carry out scalability and biodegradability tests of the materials in order to better understand the applicability of pilot plants to aquaculture systems.

4. Experimental Section

Materials: Fresh yellow soybean (*Glycine max*) seeds were purchased by Del Prete s.r.l. (Fondi, LT, Italy) and stored at room temperature before use. Medium molecular weight chitosan (Mw = 190–310 KDa, 75–85% N-deacetylation degree), gelatine from cold-water fish skin, methacrylic anhydride (MA, 94%), acetic acid (96%), the photoinitiator Irgacure 2959, alginic acid sodium salt (99%), chloroacetic acid (>99%), isopropyl alcohol, calcium chloride ($CaCl_2$, >93%), disodium ethylenediaminetetraacetate (Na_2EDTA, 99%), hydrochloric acid (HCl, 37%) and sodium hydroxide (NaOH, >98%) were purchased from Sigma-Aldrich (Milano, Italy). Elements standard solutions were prepared from concentrated (1000 and 10 000 mg L^{-1}) stock solutions (Sigma-Aldrich TraceCERT St. Louis, MO, USA) and diluted to the selected concentrations with ultra-pure water, i.e., water purified in a Milli-Q system and having a resistivity of 18.2 MΩ•cm.

Cellulose Isolation from Soybean Hulls: For carboxymethylcellulose-alginate hydrogels preparation, a waste-derived cellulose was employed and chemically modified. The biopolymer was isolated from soybean hulls, previously subjected to the extraction of soybean peroxidase enzyme,[60] following the method proposed by Tummino et al.[61] and Rigoletto et al.[53] In brief, the biomass was treated with a 2% w/v sodium hydroxide solution (solid–liquid ratio 1:10) for two h at 80 °C, then washed with distilled water up to a neutral pH value and dried at 60 °C. Successively, the pre-treated pulp was subjected to acid hydrolysis with 1 M HCl (solid–liquid ratio 1:10) at 80 °C for two h, then washed with distilled water up to a neutral pH and dried at 60 °C. Finally, the pulp was treated once more with the 2% w/v of NaOH solution (solid–liquid ratio 1:10), washed, and dried at 60 °C again to obtain the final product.

Synthesis of Carboxymethylcellulose and Hydrogel Preparation: Carboxymethylcellulose was synthesized through the acetylation of previously obtained cellulose following the method proposed by Robles Barros et al.[62] with minor modifications.

This procedure consists of two steps: alkalinization and etherification. For the first stage, 3 g of cellulose was homogenized in 80 mL of isopropyl alcohol under stirring for 30 min, followed by the addition of 10 mL of 50% w/v NaOH solution. After 30 min of stirring the suspension was heated up to 63 °C and 6.3 g of chloroacetic acid was added for the etherification stage. At the end of the reaction (190 min), the modified cellulose was recovered by filtration and washed with 70% ethanol. Finally, the CMC was left under stirring in ethanol for 30 min, washed again with methanol, and dried in an oven at 50 °C.

The degree of substitution (DS) was evaluated according to Aguir and M'Henni.[63] 1 g of CMC was mineralized at 600 °C for 4 h and the obtained ash was cooled to room temperature and dissolved in 25 mL of hot distilled water (80 °C). The solution was titrated with 0.1N (0.05 M) H_2SO_4 in the presence of methyl orange. The obtained reddish solution was heated to remove dissolved CO_2 until it reached a yellow color. A second titration was performed with H_2SO_4.

The DS could be calculated using the Equation (2)

$$DS = \frac{(0.162 \times B)}{(1 - 0.08 \times B)} \quad B = 0.1 \times \frac{V}{m} \tag{2}$$

where 0.162 is the molar mass of the glucose unit (AGU) expressed in kg mol^{-1}, 0.08 is the molar mass of sodium acetate group substituted in the cellulose (kg mol^{-1}); 0.1 is the normality of sulfuric acid solution; m is the mass (g) of the CMC samples mineralized and V is the total volume (mL) of H_2SO_4 used for the titration.

CMC-alginate hydrogels (HY-ACMC) were prepared through gelation in calcium chloride solution and a CMC-alginate ratio of 1:3 was chosen. 0.225 g of sodium alginate and 0.18 g of CMC were dissolved in 12 mL of distilled water and left under stirring until complete homogenization. Successively, the viscous solution was dripped in 0.2 M $CaCl_2$ solution with a plastic syringe in order to obtain beads.[53] The resulting spherical hydrogels were left in the gelling solution for 3 days, then washed with distilled water and dried at 105 °C overnight.

Synthesis of Methacrylated Chitosan and Hydrogel Preparation: The methacrylation reaction of chitosan was carried out as previously described.[19] CHI was solubilized in 2% w/w acetic acid aqueous solution with a concentration of 1.5% wt. Then, MA was added dropwise with 1:20 molar ratio between aminoglucose moieties of CHI and MA. The solution was stirred for 4 h at 50 °C. The product solution was transferred into a dialysis tubing cellulose membrane and dialyzed against distilled water for 4 days. The dialysis was performed to remove the excess of MA and the resulting by-products from the methacrylation reaction. After this time, the product was freeze-dried to remove water and obtain methacrylated chitosan (MCHI).

In order to obtain a 3D polymeric network, the chitosan-based hydrogels (HY-MCHI) were produced by means of radical photopolymerization.[19] A total of 1.5% w/w of MCHI was dissolved in 2% w/w acetic acid solution, then 2 phr (per hundred resin) of Irgacure 2959 was added. Once the mixture was homogenous, the formulation was poured into a cylinder-shape silicon mold (1 cm in diameter, 1 cm in height) and irradiated for 5 min with UV light (90 mW cm^{-2}) using a Hamamatsu LC8 lamp with 8 mm light guide and spectral distribution range of 240–400 nm. Finally, the produced hydrogels were air-dried.

Synthesis of Methacrylated Gelatine and Hydrogel Preparation: Gelatine from fish skin was methacrylated following a previously reported procedure.[16,18] First, 30% w/w of GEL was solubilized in distilled water at 50 °C. After the complete homogeneity was achieved, 0.6 g of MA for 1 g of GEL was added dropwise. The reaction was conducted for 4 h at 50 °C under stirring conditions and at pH 8 by the addition of 3 M NaOH solution. The resulting solution was dialyzed against distilled water for 3 days and then freeze-dried to obtain the methacrylated gelatin (MGEL).

As well as HY-MCHI, also the gelatine-based hydrogels (HY-MGEL) were obtained through radical UV-curing.[18] MGEL (30% wt) was dissolved in distilled water before adding 1 phr of Irgacure 2959. Subsequently, the liquid solution was transferred to a rectangular silicone mold with thickness equal to 1 mm. The samples were irradiated for 1 min with UV light (90 mW cm^{-2}) by means of the same Hamamatsu lamp mentioned above, then they were air-dried.

Hydrogels Characterization: The successful methacrylation reaction of CHI and GEL was confirmed by ATR-FTIR. Thermo Scientific Nicolet iS50 FTIR spectrometer (Thermo Fisher Scientific, Milano, Italy) equipped with a diamond crystal ATR accessory and a resolution of 4 cm^{-1} in the range of 4000–600 cm^{-1} was used. To investigate the success of cellulose carboxymethylation reaction a Spectrum Two UATR spectrometer (PerkinElmer) has been employed in the same range.

The surface charge of hydrogels was investigated through the zeta (ζ) potential measurement. ≈500 mg of swelled samples were introduced into a cylindrical cell. The ζ potential was evaluated as a function of pH in 0.001 M KCl electrolyte solution. 0.05 M HCl and 0.05 M NaOH solutions were added to change the pH for titration in the acid and alkaline range, respectively. Four ramps were carried out for each point collected. An electrokinetic analyzer (SurPASS, Anton Paar) equipped with an automatic titration unit was used.

The swelling behavior of the hydrogels was investigated through a gravimetric method. Dried hydrogels were soaked in distilled water at room temperature and weight gain was monitored until it remained constant. The swelling ratio (Sw) was calculated with Equation (3) where w_s and w_d represent the weight of the swollen and dry samples, respectively.

$$Sw = \frac{w_s - w_d}{w_d} \tag{3}$$

PTEs Adsorption Test in Ultra-Pure and Real Water Samples: To evaluate the influence of PTEs initial concentration and pH on the adsorption capacity, adsorption experiments were carried out in multi-element solutions at specific concentrations and fixed pH values.

PTEs removal percentage (R%) and adsorbent capacities (q_e), expressed in mg of PTEs adsorbed for g of adsorbent, have been calculated using Equation (4) and Equation (5).

$$R\% = 100 - \left(\frac{C}{C_0} \times 100\right) \tag{4}$$

$$q_e = \frac{(C_0 - C) \times V}{W_{HY}} \tag{5}$$

where C_0 is the PTE's initial molar concentration, C is the PTE's molar concentration at each contact time, V is the volume (L) of PTEs multi-element solution and W_{HY} is the weight (g) of adsorbent used for adsorption experiments.

The influence of PTEs initial concentration was investigated employing multi-element stock solutions prepared in ultrapure water at the concentration of 10^{-6}, 10^{-5}, and 10^{-4} M (for each element). Adsorption experiments were carried out at pH 5 with an adsorbent dose of 1 g L^{-1}. PTEs' concentration has been determined at different contact times (in the range 0–24 h) by Inductively Coupled Plasma Atomic Emission Spectrometry (ICP-AES, PerkinElmer Optima 7000 DV spectrometer) or by Inductively Coupled Plasma Mass Spectrometry (ICP-MS, Agilent 7500ce) as a function of initial concentration.

The influence of pH on adsorbents' efficiency was evaluated by performing adsorption experiments in a 10^{-5} M multi-element solution, using an adsorbent dose of 1 g L^{-1} at pH 3.5, 5, and 7. PTEs' concentrations were determined at different contact times by ICP-AES.

Contaminants' speciation was studied as well. For this purpose, a modeling technique was employed, assuming that only hydrolysis equilibria occur as expected on the basis of the composition of solutions used during the test. Speciation diagrams for each metal cation were obtained by PyES software[64] taking into consideration: (i) thermodynamic formation constants (infinite dilution condition)[65]; (ii) temperature of 25 °C; (iii) metal concentration 10^{-5} M; (iv) pH range between 3 and 8.

Two different water samples from aquaculture farms have been employed as matrix to study adsorption capacity in real conditions: Italian koi carps' aquaculture water from the Agrozootechnics Centre "Tetto Frati" (Carmagnola – Turin, Italy) and Danish aquaculture water from Ultraaqua (Aalborg, Denmark). After the sampling, the water samples were stored at −18 °C until their use.

Water samples were then thawed and filtered with 0.45 µm cellulose acetate filters, their pH and hardness were measured. Successively, water samples were acidified with HNO_3 (0.1%), and their original PTEs' content was determined by ICP-MS spectrometry. For the adsorption experiments, water samples thawed, not-filtered, and not-acidified were used as matrix for multi-element PTEs' solutions preparation.

Each element was added at a concentration close to its Italian legal limit (50 µg L^{-1} As; 22 or 40 µg L^{-1} Cu; 10 or 20 µg L^{-1} Pb; 50 or 75 µg L^{-1} Ni and 200 or 300 µg L^{-1} Zn, as reported in Table S3, Supporting Information) as function of water hardness (Italian Legislative Decree n°152/2006, Annex 2, Part III, Section B). For Cd and Hg a concentration of 5 µg L^{-1}, higher than their legal limits (2.5 and 0.5 µg L^{-1} respectively) was selected.

As for the previous experiments, 1 g L^{-1} of each adsorbent was employed, and PTEs' concentrations were determined at different contact times by ICP-AES. A range between 0 and 180 min was selected as this was sufficient to reach PTEs removals close to equilibrium conditions.

Hydrogels Regeneration and Reuse: Different regeneration methods were investigated in order to evaluate the possibility to use the hydrogels for multiple successive adsorption-desorption cycles. For this purpose, preliminary tests with HY-ACMC have been done using HCl 0.01 M; HCl 0.1 M, and Na_2EDTA 0.01 M as PTEs desorption mediums.[55,56,66,67]

At the end of each adsorption test, HY-ACMC hydrogels were washed with 10 mL of ultrapure water and immersed in 20 mL of desorption solution. Released PTEs' concentrations both in the washing water and in the regeneration solutions were determined at different times (0–240 min) by ICP-AES spectrometry.

In the second phase, multiple desorption methods were studied. At the end of the adsorption tests HY-ACMC hydrogels were immersed in 20 mL of each desorption solution for 30 min, then filtered and added in 20 mL of fresh desorption solution. This treatment was repeated two more times. The four volumes of regeneration medium were analyzed by ICP-AES spectrometry to evaluate the PTEs released concentrations.

Na_2EDTA 0.01 M was selected as the best regeneration solution and was also tested on HY-MGEL and HY-MCHI. Classic adsorption experiments (10^{-5} M multi-element solution, pH 5, 1 g L^{-1} of adsorbent) were carried out and PTEs concentrations were monitored at fixed adsorption time (0, 60, 120, and 180 min) by ICP-AES spectrometry. At the end of each experiment, the hydrogels were washed with 10 mL of ultrapure water and subjected to 3 subsequent regeneration treatments, each one lasting ≈30 min, with 20 mL of Na_2EDTA 0.01 M. PTEs released concentrations were monitored by ICP-AES spectrometry.

After the regeneration process, the hydrogels have been used for two other adsorption cycles interspersed with 3 regeneration cycles.

The desorption (Des), expressed in mg g^{-1}, and desorption percentages (Des%) were calculated using Equation (6) and Equations (7) respectively.

$$Des = \frac{\left(C \times V_{reg}\right)}{W_{HY}} \tag{6}$$

$$Des\% = \frac{W_{PTE-des}}{W_{PTE-ads}} \times 100 \tag{7}$$

where V_{reg} (L) is the volume of regeneration solution (HCl 0.01 M, HCl 0.1 M, or Na_2EDTA 0.01 M), W_{HY} (g) is the dried weight of adsorbent, C is the PTEs molar concentration at each regeneration treatment time, $W_{PTE\text{-}ads}$ is the weight (mg) of each PTE adsorbed at the end of the adsorption experiment, $W_{PTE\text{-}des}$ is the weight (mg) of each PTE desorbed at each regeneration treatment time.

Supporting Information

Supporting Information is available from the Wiley Online Library or from the author.

Acknowledgements

M.R. and R.S. contributed equally to this work. This research received funding from the European Union's Horizon 2020 research and innovation program under the Marie Skłodowska-Curie grant agreement no. 101007578 (SusWater). M. Rigoletto, E. Laurenti, P. Calza, S. Berto, and M. Malandrino acknowledge support from Project CH4.0 under MUR (Italian Ministry for the University) program "Dipartimenti di Eccellenza 2023–2027" (CUP: D13C22003520001). MUR is acknowledged for funding R. Sesia's Ph.D. fellowship (MUR – D.M.1061/2021 – Dottorati di ricerca su tematiche green e dell'innovazione: nuove risorse dal PON Ricerca e Innovazione).

Open access publishing facilitated by Universita degli Studi di Torino, as part of the Wiley - CRUI-CARE agreement.

Conflict of Interest

The authors declare no conflict of interest.

Data Availability Statement

The data that support the findings of this study are available from the corresponding author upon reasonable request.

Keywords

adsorption, aquaculture, environmental chemistry, polymers, water chemistry

Received: November 27, 2024
Revised: April 7, 2025
Published online: April 18, 2025

[1] FAO, The State of World Fisheries and Aquaculture: Towards Blue Transformation, Rome, Italy, **2022**.
[2] E. C. Emenike, K. O. Iwuozor, S. U. Anidiobi, *Biol. Trace Elem. Res.* **2022**, *200*, 4476.
[3] S.-A. Strungaru, M. Nicoara, C. Teodosiu, E. Baltag, C. Ciobanu, G. Plavan, *Chemosphere* **2018**, *207*, 192.
[4] N. Agasti, *Curr. Res. Green and Sustainable Chem.* **2021**, *4*, 100088.
[5] E. I. Ugwu, O. Tursunov, D. Kodirov, L. M. Shaker, A. A. Al-Amiery, I. Yangibaeva, F. Shavkarov, *IOP Conf. Ser.: Earth Environ. Sci.* **2020**, *614*, 012166.
[6] P. Kanmani, J. Aravind, M. Kamaraj, P. Sureshbabu, S. Karthikeyan, *Bioresour. Technol.* **2017**, *242*, 295.
[7] F. G. L. Medeiros Borsagli, A. A. P. Mansur, P. Chagas, L. C. A. Oliveira, H. S. Mansur, *React. Funct. Polym.* **2015**, *97*, 37.
[8] M. Zanon, A. Chiappone, N. Garino, M. Canta, F. Frascella, M. Hakkarainen, C. F. Pirri, M. Sangermano, *Mater. Adv.* **2022**, *3*, 514.
[9] M. Zanon, L. Montalvillo-Jiménez, P. Bosch, R. Cue-López, E. Martínez-Campos, M. Sangermano, A. Chiappone, *Polymers* **2022**, *14*, 4709.
[10] C. Noè, A. Cosola, A. Chiappone, M. Hakkarainen, H. Grützmacher, M. Sangermano, *Polymer* **2021**, *235*, 124257.
[11] K. Y. Lee, D. J. Mooney, *Prog. Polym. Sci.* **2012**, *37*, 106.
[12] P. Mehta, M. Sharma, M. Devi, *J. Mech. Behav. Biomed. Mater.* **2023**, *147*, 106145.
[13] R. Sesia, A. G. Cardone, S. Ferraris, S. Spriano, M. Sangermano, *Prog. Org. Coat.* **2024**, *189*, 108311.
[14] L. Pezzana, G. Melilli, N. Guigo, N. Sbirrazzuoli, M. Sangermano, *Macromol. Chem. Phys.* **2023**, *224*, 2200012.
[15] M. Sangermano, N. Razza, J. V. Crivello, *Macromol. Mater. Eng.* **2014**, *299*, 775.
[16] M. Vigata, C. Meinert, S. Pahoff, N. Bock, D. W. Hutmacher, *Polymers* **2020**, *12*, 501.
[17] L. Song, F. Liu, C. Zhu, A. Li, *Chem. Eng. J.* **2019**, *369*, 641.
[18] C. Noè, M. Zanon, A. Arencibia, M.-J. López-Muñoz, N. Fernández de Paz, P. Calza, M. Sangermano, *Polymers* **2022**, *14*, 1268.
[19] R. Sesia, S. Ferraris, M. Sangermano, S. Spriano, *Polymers* **2022**, *14*, 4645.
[20] K. J. Goudie, S. J. McCreath, J. A. Parkinson, C. M. Davidson, J. J. Liggat, *J. Polym. Sci.* **2023**, *61*, 2316.
[21] N. Benbettaïeb, R. Mahfoudh, S. Moundanga, C.-H. Brachais, O. Chambin, F. Debeaufort, *Int. J. Biol. Macromol.* **2020**, *160*, 780.
[22] F.-Y. Shih, I.-J. Su, L.-L. Chu, X. Lin, S.-C. Kuo, Y.-C. Hou, Y.-T. Chiang, *Int. J. Mol. Sci.* **2018**, *19*, 3625.
[23] Y. Zhu, B. Bhandari, S. Prakash, *Food Hydrocolloids* **2018**, *84*, 292.
[24] N. Li, R. Bai, *Sep. Purif. Technol.* **2005**, *42*, 237.
[25] S. Zhao, F. Zhou, L. Li, M. Cao, D. Zuo, H. Liu, *Composites, Part B* **2012**, *43*, 1570.
[26] J. Borges-Vilches, T. Figueroa, S. Guajardo, M. Meléndrez, K. Fernández, *Polymer* **2020**, *208*, 122951.
[27] F. Zhu, L. Chen, Q. Feng, *Prog. Org. Coat.* **2022**, *163*, 106688.
[28] L. Wang, X. Liu, X. Wang, X. Yang, L. Lu, *J. Mater. Sci.* **2011**, *46*, 634.
[29] B. Wang, X. Yang, L. Ma, L. Zhai, J. Xuan, C. Liu, Z. Bai, *Sep. Purif. Technol.* **2020**, *231*, 115922.

[30] B. He, H. Xue, *Water Qual. Res. J.* **2015**, *50*, 314.
[31] L. Peng, Y. Peng, A. Primo, H. García, *ACS Appl. Mater. Interfaces* **2021**, *13*, 13499.
[32] C. Dong, W. Chen, C. Liu, *Bioresour. Technol.* **2014**, *170*, 239.
[33] C.-C. Chung, H.-W. Chen, H.-T. Wu, *Appl. Sci.* **2022**, *12*, 5249.
[34] L. P. H. Bastos, C. W. P. de Carvalho, E. E. Garcia-Rojas, *Int. J. Biol. Macromol.* **2018**, *120*, 332.
[35] C. Liu, Z. Zhang, Q. Kong, R. Zhang, X. Yang, *R. S. C. Adv* **2019**, *9*, 10004.
[36] T. Cai, Z. Yang, H. Li, H. Yang, A. Li, R. Cheng, *Cellulose* **2013**, *20*, 2605.
[37] B. Lam, S. Déon, N. Morin-Crini, G. Crini, P. Fievet, *J. Cleaner Prod.* **2018**, *171*, 927.
[38] L. Zhang, Y. Zeng, Z. Cheng, *J. Mol. Liq.* **2016**, *214*, 175.
[39] W. Zhan, C. Xu, G. Qian, G. Huang, X. Tang, B. Lin, *R. S. C. Adv* **2018**, *8*, 18723.
[40] M. Zhang, Q. Yin, X. Ji, F. Wang, X. Gao, M. Zhao, *Sci. Rep.* **2020**, *10*, 3285.
[41] Z. Sun, Y. Yin, Y. An, C. Deng, Z. Wei, Z. Jiang, X. Duan, X. Xu, J. Chen, *J. Environ. Chem. Eng.* **2022**, *10*, 108179.
[42] J. Singh, A. N. Srivastav, N. Singh, A. Singh, J. Singh, A. N. Srivastav, N. Singh, A. Singh, in *Stability and Applications of Coordination Compounds*, IntechOpen, London, UK **2019**.
[43] G. Zhou, J. Luo, C. Liu, L. Chu, J. Ma, Y. Tang, Z. Zeng, S. Luo, *Water Res.* **2016**, *89*, 151.
[44] J. Ma, Y. Liu, O. Ali, Y. Wei, S. Zhang, Y. Zhang, T. Cai, C. Liu, S. Luo, *J. Hazard. Mater.* **2018**, *344*, 1034.
[45] M. A. H. Badsha, M. Khan, B. Wu, A. Kumar, I. M. C. Lo, *J. Hazard. Mater.* **2021**, *408*, 124463.
[46] R. Dubey, J. Bajpai, A. K. Bajpai, *Environ. Nanotechnol. Monit. Manage.* **2016**, *6*, 32.
[47] M. Monier, D. A. Abdel-Latif, *Chem. Eng. J.* **2013**, *221*, 452.
[48] F. A. Alakhras, K. A. Dari, M. S. Mubarak, *J. Appl. Polym. Sci.* **2005**, *97*, 691.
[49] G. Cassone, D. Chillé, C. Foti, O. Giuffré, R. C. Ponterio, J. Sponer, F. Saija, *Phys. Chem. Chem. Phys.* **2018**, *20*, 23272.
[50] Y. Hu, X. Jiang, Y. Ding, H. Ge, Y. Yuan, C. Yang, *Biomaterials* **2002**, *23*, 3193.
[51] W.-B. Wang, D.-J. Huang, Y.-R. Kang, A.-Q. Wang, *Colloids Surf., B* **2013**, *106*, 51.
[52] N. Esfandiar, R. Suri, E. R. McKenzie, *J. Hazard. Mater.* **2022**, *423*, 126938.
[53] M. Rigoletto, P. Calza, A. S. da Cunha, V. Sederino, D. Fabbri, M. L. Tummino, E. Laurenti, *React. Chem. Eng.* **2023**, *8*, 1629.
[54] H. Wang, Z. Wang, R. Yue, F. Gao, R. Ren, J. Wei, X. Wang, Z. Kong, *Chem. Eng. J.* **2020**, *383*, 123107.
[55] H. Isawi, *Arabian J. Chem.* **2020**, *13*, 5691.
[56] T. V. J. Charpentier, A. Neville, J. L. Lanigan, R. Barker, M. J. Smith, T. Richardson, *A. C. S. Omega* **2016**, *1*, 77.
[57] D. R. Sahoo, T. Biswal, *SN Appl. Sci.* **2021**, *3*, 30.
[58] R. M. C. Dawson, D. C. Elliott, W. H. Elliott, *Data for Biochemical Research*, Oxford University Press, Oxford, UK **1989**.
[59] C. Kim, S.-K. Ong, *J. Hazard. Mater.* **1999**, *69*, 273.
[60] P. Calza, D. Zacchigna, E. Laurenti, *Environ. Sci. Pollut. Res.* **2016**, *23*, 23742.
[61] M. L. Tummino, E. Laurenti, P. Bracco, C. Cecone, V. L. Parola, C. Vineis, M. L. Testa, *Cellulose* **2023**, *30*, 7805.
[62] P. J. Robles Barros, D. P. Ramirez Ascheri, M. L. Siqueira Santos, C. C. Morais, J. L. Ramirez Ascheri, R. Signini, D. M. dos Santos, A. J. de Campos, I. Alessandro Devilla, *Int. J. Biol. Macromol.* **2020**, *144*, 208.
[63] C. Aguir, M. F. M'Henni, *J. Appl. Polym. Sci.* **2006**, *99*, 1808.
[64] L. Castellino, E. Alladio, S. Bertinetti, G. Lando, C. De Stefano, S. Blasco, E. García-España, S. Gama, S. Berto, D. Milea, *Chemom. Intell. Lab. Syst.* **2023**, *239*, 104860.
[65] The IUPAC Stability Constant Database, Version 5.84. Academic Software. Sourby Old Farm, Timble, Otley, Yorks, LS21 2PW. In SC-Database.
[66] H. Fan, X. Ma, S. Zhou, J. Huang, Y. Liu, Y. Liu, *Carbohydr. Polym.* **2019**, *213*, 39.
[67] Z.-H. Hu, A. M. Omer, X. Ouyang, D. Yu, *Int. J. Biol. Macromol.* **2018**, *108*, 149.